https://doi.org/10.5194/acp-2020-920
Preprint. Discussion started: 14 November 2020

Atmospheric Chemistry and Physics Discussions
Open Access
EGU

Effectiveness of emission control to reduce $PM_{2.5}$ pollution of Central China during winter haze episodes under various potential synoptic controls

Yingying Yan [1#], Yue Zhou [2#], Shaofei Kong [1,4*], Jintai Lin [3], Jian Wu[1,4], Huang Zheng [1,4], Zexuan Zhang [1,4], Yongqing Bai [2], Zhang Ling [2], Dantong Liu [5], Tianliang Zhao [6]

[1] Department of Atmospheric Sciences, School of Environmental Studies, China University of Geosciences, Wuhan, 430074, China

[2] Hubei Key Laboratory for Heavy Rain Monitoring and Warning Research, Institute of Heavy Rain, China Meteorological Administration, Wuhan 430205, China

[3] Laboratory for Climate and Ocean-Atmosphere Studies, Department of Atmospheric and Oceanic Sciences, School of Physics, Peking University, Beijing 100871, China

[4] Department of Environmental Science and Engineering, School of Environmental Studies, China University of Geosciences, Wuhan, 430074, China

[5] Department of Atmospheric Sciences, School of Earth Sciences, Zhejiang University, Hangzhou, Zhejiang, China

[6] School of Atmospheric Physics, Nanjing University of Information Science and Technology, Nanjing, 210044, China

Correspondence to: Shaofei Kong (kongshaofei@cug.edu.cn)

[#] Contributed equally to this work

Abstract

Currently solving the severe particle pollution in autumn and winter is the key to further improve the air quality of China. The source contributions and transboundary transport of fine particles ($PM_{2.5}$) in pollution episodes are closely related to large-scale or synoptic-scale atmospheric circulation. Under different synoptic conditions, how to effectively reduce emissions to control haze pollution is rarely reported. In this study, we classify the synoptic conditions over Central China from 2013 to 2018 by using Lamb-Jenkension method and the NCEP/NCAR FNL operational global analysis data.

https://doi.org/10.5194/acp-2020-920
Preprint. Discussion started: 14 November 2020

Atmospheric Chemistry and Physics Discussions

The effectiveness of emission control to reduce $PM_{2.5}$ pollution during winter haze episodes under potential synoptic controls is simulated by GEOS-Chem model. Among the ten identified synoptic patterns, four types account for 87% of the total pollution days. Two typical synoptic modes of them are characterized by small surface wind speed and stable weather conditions/high relative humidity (A/C-type) over Central China due to a high-pressure system/a southwest trough low-pressure system, blocking pollutants dispersion. Sensitivity simulations show that these two heavy pollution processes are mainly contributed by local emission sources with ~82% for A-type and ~85% for C-type, respectively. The other two patterns lead to pollution of transportation characteristics affected by northerly/southerly winds (NW/SW-type), carrying air pollution from northern/southern China to Central China. The contribution of pollution transportation from North/South China is 36.9%/7.6% of $PM_{2.5}$ and local emission sources contribute 41%/69%. We also estimate the effectiveness of emission reduction in these four typical severe pollution synoptic processes. By only reducing SO_2 and NO_x emission and not controlling NH_3, the enhanced nitrate counteracts the effect of sulfate reduction on $PM_{2.5}$ mitigations with less than 4% decrease in $PM_{2.5}$. In addition, to effectively mitigate haze pollution in NW/SW-type synoptic controlled episodes, local emission control actions should be in coordination with regional collaborative actions.

1 Introduction

The regional pollution of fine particles ($PM_{2.5}$) has attracted worldwide attention in the public and in the scientific community (Cheng et al., 2016; Li et al., 2017c; Lin et al., 2018; Bi et al., 2019) due to its detrimental effect on visibility (Wang et al., 2020) and public health (Agarwal et al., 2017; Zhang et al., 2017). The $PM_{2.5}$ pollution in China has been continuously alleviating since 2013 as the implication of the Air Pollution Prevention and Control Action Plan (Zheng et al., 2018; Zhang et al., 2019), especially in the Beijing-Tianjin-Hebei region (BTH) (Li et al., 2017b; Cheng et al.,

https://doi.org/10.5194/acp-2020-920
Preprint. Discussion started: 14 November 2020

2019), the Yangtze River Delta (YRD) region and the Pearl River Delta (PRD) region. However, severe particle pollution still occurs frequently in autumn and winter, which is the major reason restricting the $PM_{2.5}$ to come up to national standard. For example, 12 extremely severe and persistent $PM_{2.5}$ pollution episodes occurred in Beijing in January 2013, February 2014, December 2015, December 2016 and January 2017 (Zhong et al., 2018; Sun et al., 2016; Wang et al., 2018). Currently, how to effectively reduce emissions in autumn and winter is the key to mitigate haze pollution in China.

The contribution of emission sources has been widely recognized as the decisive factor of $PM_{2.5}$ pollution over urban agglomerations, including industrial exhaust, urban transportation, residential emission, power plants, agricultural activities, and bio-combustion (Huang et al., 2014; Tian et al., 2016; Wu et al., 2018; An et al., 2019). While the outbreak, persistence and dissipation of particle pollution generally depends on the meteorological conditions and regional synoptic patterns, controlled by the large-scale or synoptic-scale atmospheric circulation (Chuang et al., 2008; Zhang et al., 2012; Russo et al., 2014; Zheng et al., 2015; Shu et al., 2017; Li et al., 2019).

Many studies have tried to reveal the relationship between synoptic patterns and severe particle pollution, and estimate the meteorological contributions to these pollution episodes. The YRD is mainly affected by pollutants transmitted from the northern and the southern China when the East Asian major trough is located at its front (Liao et al., 2017; Shu et al., 2017; Li et al., 2019). Liao et al. (2020) has confirmed that the relative position of the PRD to high-pressure systems imposed significant impacts on the diffusion conditions and the $PM_{2.5}$ distributions in the PRD region. For North China Plain (NCP), high frequency of stagnant weather accompanied by small pressure gradient and near-surface wind speed, and shallow mixing layer is a major reason of aerosol pollution over this region in winter (He et al., 2018). The aerosol pollution formation process in Sichuan Basin is often controlled by the large scale high-pressure circulation at sea level (Sun et al., 2020). In the Guanzhong basin, pollution event is generally governed by both the large-scale synoptic situation and the small-scale local

https://doi.org/10.5194/acp-2020-920
Preprint. Discussion started: 14 November 2020

circulation. The downhill wind not only forms a convergence zone in the basin, but also makes pollutants flow back from the mountain region to the basin (Bei et al., 2017). Leung et al. (2018) also find strong correlations of daily $PM_{2.5}$ variability with several synoptic patterns, including monsoon flows and cold front channels in northern China related to the Siberian High, onshore flows in eastern China, and frontal rainstorms in southern China. These previous studies have highlighted that different levels of $PM_{2.5}$ pollution are closely related to the dominant synoptic patterns in different regions, and they attribute the large spatial variability of pollution to the regional transport contributions, not only the different local sources of $PM_{2.5}$. However, under different synoptic conditions, how to effectively reduce local and regional emissions to control haze pollution is rarely reported.

Various key regions have issued the emergency preplan against the winter haze episodes, while these schemes can only be targeted at a certain city (The People's Government of Beijing Municipality, 2018; The People's Government of Shanghai Municipality, 2018) or a certain urban agglomeration (The People's Government of Guangdong Province, 2014). They always have no binding forces on the larger scale emission reduction outside of a specific region, which is not conducive to effective $PM_{2.5}$ mitigations. Moreover, current emission reduction policies in China mainly aimed at sulfur dioxide (SO_2) and nitrogen dioxide (NO_2), ignoring the effective emission reduction on ammonia (NH_3). Compared to remarkable reduction in SO_2, NO_2, and primary PM emissions, NH_3 emissions has remained stable during 2014–2018 in China (Zheng et al., 2018). Given the important role of NH_3 in secondary inorganic aerosol formation (Geng et al., 2019; Liu et al., 2019), cutting NH_3 emissions should be proposed as a next-step mitigation strategy. Therefore, for $PM_{2.5}$ mitigations during winter haze episodes in a specific region forced by potential synoptic controls, whether the air pollution emergency management and control schemes are effective and how to improve them has become an urgent scientific question to be answered.

In order to investigate the effectiveness of emission control to reduce $PM_{2.5}$ pollution during winter haze episodes under various potential synoptic controls, we take the severe particle pollution of winter haze episodes over Jingzhou, the hinterland of Yangtze River middle basin in Central China, as an example. Jingzhou is geographically surrounded by major haze pollution regions, the SCB to the west, the PRD to the south, the YRD to the east, and the NCP to the north (Fig. 1). As a regional pollutant transport hub with sub basin topography, Central China is a region of transportation-pollution characteristics affected by two reported transport pathways from the vast flatland in central eastern China (Yu et al., 2020) and from the NCP region (Zheng et al., 2019a). In combination with high anthropogenic emissions (Wu et al., 2018) and secondary aerosol formation (Huang et al., 2020), Central China often suffers severe pollution episodes in winter caused by $PM_{2.5}$ (Gong et al., 2015; Xu et al., 2017). In this study, we conduct the circulation classification to differentiate the synoptic modes during the severe particle pollution episodes in winter over Central China from 2013 to 2018 by using Lamb-Jenkension method. Then we simulate the $PM_{2.5}$ chemical components, and the contributions of local sources as well as transboundary transport of $PM_{2.5}$ under different synoptic conditions. Finally, the effectiveness of emission reduction in main potential synoptic patterns are evaluated by GEOS-Chem model simulations. This study could provide reference for emission control of severe winter haze pollution under different weather types, and provide basis for regional air quality policy-making.

2 Data and Methods

2.1 Data

Hourly mass concentrations of $PM_{2.5}$ at Jingzhou (112.18°E, 30.33°N, 33.7 m) from November 2013 to December 2018 are obtained from Hubei Environmental Monitoring Central Station (http://sthjt.hubei.gov.cn/). We screen the pollution days

https://doi.org/10.5194/acp-2020-920
Preprint. Discussion started: 14 November 2020

with daily mean $PM_{2.5}$ concentrations larger than 150 μg/m^3 for circulation classification.

Figure 1

The meteorological data of surface observations at Jingzhou, including ambient temperature, relative humidity, wind speed, wind direction and atmospheric pressure, are obtained from Hubei Meteorological Information and Technology Support Center (http://hb.cma.gov.cn/qxfw/index.html). The data used in this study are from November 2013 to February 2014, in which four severe particle pollution events occurred in succession over Central China (Fig. S1).

We use the daily mean sea level pressures (SLP) from the National Centers for Environmental Prediction/National Center for Atmospheric Research (NCEP/NCAR) Final (FNL) Operational Global Analysis data (horizontal resolution: 1° × 1°; temporal resolution: 6 hours; https://rda.ucar.edu/datasets/ds083.3/) to conduct the classification of Lamb-Jenkension circulation types.

2.2 Lamb-Jenkension Circulation Classification

The atmospheric circulation classification adopts the Lamb-Jenkension method proposed by Lamb et al. (1950) and developed by Jenkension et al. (1977). This method is a combination of subjective and objective methods, overcoming the weaknesses of their respective (Trigo and DaCamara, 2000) and leading to better synoptic significance (Pope et al., 2015).

To calculate the circulation types of Jingzhou, we mark total 16 points (97.5°E-127.5°E, 20°N-40°N) by every 10 longitudes and 5 latitudes and the center point located at 112.5° E and 30° N (Fig. S2). Using the sea level pressure of 16 points, we calculate six circulation indexes by scheme of central difference:

$$u = 0.5[P(12) + P(13) - P(4) - P(5)]$$

(1)

https://doi.org/10.5194/acp-2020-920
Preprint. Discussion started: 14 November 2020

$$v = \frac{1}{\cos a} \times \frac{1}{4}[P(4) + 2P(9) + P(13) - P(4) - 2P(8) - P(12)]$$

(2)

$$V = \sqrt{u^2 + v^2}$$

(3)

$$\xi_u = \frac{\sin\alpha}{2\sin\alpha_1}[P(15) + P(16) - P(8) - P(9)] - \frac{\sin\alpha}{2\sin\alpha_2}[P(8) + P(9) - P(1) - P(2)]$$

(4)

$$\xi_v = \frac{1}{8\cos^2\alpha}[P(6) + 2P(10) + P(14) - P(5) - 2P(9) - P(13) + P(3) + 2P(7) + P(11) - P(4) - 2P(8) - P(12)]$$

(5)

$$\xi = \xi_u + \xi_v$$

(6)

Where $P(n)(n = 1, 2, 3 \cdots 16)$ is the sea level pressure at the n^{th} point; α, α_1 and α_2 are the latitude values of points C, A_1 and A_2, respectively; V is the geostrophic wind, u and v are the latitudinal and meridional components of the geostrophic wind; ξ is the geostrophic vorticity; ξ_u is the u meridional gradient, and ξ_v is the v latitudinal gradient.

Taking the latitude of the center point as the reference frame, the unit of six circulation indexes is $hPa/(10^o lon)$, the direction of geostrophic wind can be determined by u and v, and cyclones and anticyclones can be determined by ξ. According to the geostrophic wind speed, wind direction and vorticity value, the circulation is divided into 10 types. The classification standard and corresponding types are shown in Table 1.

Table 1

https://doi.org/10.5194/acp-2020-920
Preprint. Discussion started: 14 November 2020

2.3 GEOS-Chem simulations

The GEOS-Chem chemistry transport model is used (http://acmg.seas.harvard.edu/geos/) to simulate the spatiotemporal distribution of $PM_{2.5}$. The nested model, covering China (70°E-140°E, 15°S-55°N), is run with a horizontal resolution of 0.25° latitude × 0.3125° longitude and 72 vertical layers. The simulations, driven by the GEOS-FP assimilated meteorological data, include detailed tropospheric Ozone-NO_x-VOCs-HO_x-aerosol chemistry. More details are shown in Yan et al. (2019). In the model, anthropogenic and natural sources are fully considered in GEOS-Chem. Table S1 shows a list of emission inventories in the model. In China, the monthly grid data of 0.25° × 0.25° from MEIC inventory (http://meicmodel.org) for CO, NO_x, SO_2 and non-methane volatile organic compounds (NMVOCs) in 2013-2014 is used. Over Central China, anthropogenic sources of these species are from our group SEEA (Source Emission and Environment Research) with the grid data of 0.1° × 0.1° (not shown). The SEEA emission inventory was developed based on the year of 2017 for the Wuhan city cluster and it has been successfully adopted for the air quality simulating and forecasting of 7th CISM Military World Games in 2019. Other emission descriptions are shown in Supplementary Sect. S1.

In order to better simulate the spatiotemporal distribution of $PM_{2.5}$ over Central China, especially in winter heavy pollution periods, the standard v11-01 of GEOS-Chem is optimized according to the actual situation in China (see details in Supplementary Sect. S2), including optimizing $PM_{2.5}$ sources and increasing the proportion of sulfate primary emission (Yan et al., 2020). The $PM_{2.5}$ primary anthropogenic emissions enhance the $PM_{2.5}$ concentrations over Central China by 5-20 μg/m^3 in winter (Fig. S3). Compared with the results before the model optimization (Fig. S4), the sulfate concentration simulated by the optimized model increased from 10-20 μg/m^3 to 30-50 μg/m^3. The concentration of $PM_{2.5}$ increased and improved.

https://doi.org/10.5194/acp-2020-920
Preprint. Discussion started: 14 November 2020

3. Results and Discussion

3.1 Classification of Potential synoptic controls (PSC)

As shown in Fig. 2, among the circulation patterns of pollution-day at Jingzhou from 2013 to 2018, the frequency of SW-type circulation is the highest, accounting for 29% of the total pollution days. The frequencies of NW-type, A-type and C-type are also high, accounting for 27%, 19% and 12%, respectively. While the other six circulation patterns are less occurred, with the frequencies less than 5%. Thus, the above four typical circulation types are considered as the main potential synoptic controls of the severe particle pollution episodes over Central China.

Figure 2

3.2 Characteristics of the four main PSC

SW-type circulation mainly occurs in winter (December, January and February). The circulation at 500 hPa is relatively flat and the whole East Asia region is affected by the westerly flow (Fig. S5a). Westerly belt fluctuates greatly at 700 hPa and the middle latitude presents two ridges and a southwest trough in Asia (Fig. S6a). Jingzhou is located in the front of a trough, prevailing the weak southwest airflow. At 850 hPa, the cold high pressure center is formed in Xinjiang of China. Warm low pressure appears in the low latitude area and weak high pressure appears in the East China Sea (Fig. 3a). In combination with the surface field, a high-low-high saddle like field forms from west to east (Fig. 4a). Such synoptic type is also the dominant weather system of eastern China (Shu et al., 2017; Yang et al., 2018). Jingzhou is located in the back of Bohai-northeast high pressure and the front of southwest warm low pressure, and it is affected by the southerly airflow, associated with small local surface wind speed (< 3 m/s).

Figure 3

https://doi.org/10.5194/acp-2020-920
Preprint. Discussion started: 14 November 2020

NW-type circulation mainly occurs in the early winter (December and January). This synoptic pattern is also reported as one of the main types to affect the aerosol distributions over eastern China (Zheng et al., 2015). Circulation at 500 hPa is controlled by one trough and one ridge, with the weak ridge located in the northwest of China and the shallow trough located in the northeast of China (Fig. S5b). The whole East Asia is affected by the westerly current. The trough and ridge at 700 hPa are deepened. Affected by the flow around the plateau and the shallow trough in the northeast, Jingzhou is located at the bottom of the shallow trough, prevailing the west-northwest airflow (Fig. S6b). At 850 hPa, the cold high pressure center is formed in Xinjiang, and Jingzhou is affected by the northerly airflow, due to being in the front of the high pressure (Fig. 3b). For the sea level pressure (SLP) field, the cold high pressure is located in the west of Mongolia and Xinjiang of China (Fig. 4b). Jingzhou is located at the weak fluctuation in the front of the high pressure, and the surface wind speed is smaller than 2 m/s.

Figure 4

A-type circulation mainly occurs in the early winter. The high-altitude circulation field is controlled by one trough and one ridge (Fig. S5c and S6c). East Asia is affected by west-northwest air flow, and the SLP is controlled by a huge high pressure, with the center located in the southwest of Baikal Lake (Fig. 4c). A surface high favors accumulation of air pollutants, especially over the regions of high pressure centers (Leung et al., 2018). Jingzhou is in the sparse pressure field in the front of the high pressure (Fig. 3c and 4c), with the average wind speed of ~1.3 m/s. The uniform west-northwest air flow at high altitude would lead to the observed lower water vapor content and less cloud amount, which is conducive to radiation cooling at night. In addition, due to the weak high pressure ridge in the north, it is not conducive to the eastward and

https://doi.org/10.5194/acp-2020-920
Preprint. Discussion started: 14 November 2020

southward movement of cold air, leading to the stable weather situation. This type is also responsible for most of the severe particulate pollution days in the BTH and YRD regions (Li et al., 2019).

C-type circulation mainly occurs in winter, spring and autumn, when the relative humidity is large with the average value of 74%. East Asia is controlled by the straight westerly flow, and the southwest shallow trough is obvious at 500 hPa (Fig. S5d). In combination with the West Pacific subtropical high extending to the west, Central China is affected by the southwest flow. Southwest trough is deepened at 700 hPa, and Jingzhou is located in front of the trough and controlled by the southwest airflow (Fig. S6d). High pressure in the south of Xinjiang and the north of Plateau is strengthened at 850 hPa, and the southwest low pressure center is formed (Fig. 3d). Jingzhou is located in the low pressure system on the SLP field (Fig. 4d), with small surface wind speed (0-3 m/s). The impact of low-pressure systems on winter heavy air pollution have also been reported in the northwest Sichuan Basin (Ning et al., 2018).

3.3 $PM_{2.5}$ and chemical components under the four main PSC in control simulations

The spatiotemporal distribution of $PM_{2.5}$ and its components under the four typical synoptic controls over Central China were simulated by optimized GEOS-Chem model (Table 2). The continuous time periods covering the synoptic controls of SW-type (18-25 November, 2013), NW-type (19-26 December, 2013), A-type (14-21 January, 2014) and C-type (26 January - 2 February, 2014) are selected. The air quality at Jingzhou during the four pollution episodes is between grade 5 ($PM_{2.5}$ > 150 μg/m^3) and grade 6 heavy pollution ($PM_{2.5}$ > 250 μg/m^3, as Fig. 5a and S1a shown). The simulation time is started at November 1st, 2013, with the first two weeks used as spin up to eliminate the impact of initial conditions.

Figure 5

https://doi.org/10.5194/acp-2020-920
Preprint. Discussion started: 14 November 2020

Atmospheric Chemistry and Physics Discussions

The daily/hourly mean $PM_{2.5}$ concentrations in the four typical heavy pollution processes simulated by the control (CON) simulation (Table 2) are compared with the observations (Fig. 5a/Fig. S1a). The model underestimates the observed $PM_{2.5}$ concentrations (by 43.3 μg/m^3 on average), especially in the high $PM_{2.5}$ periods (by 116.8 μg/m^3 at the maximum occurring in November 21-23, 2013). The possible causes for underestimation are insufficient resolution of the model (Yan et al., 2014), emission errors (Lin et al., 2016), meteorological field deviations (Liu et al., 2018) and imperfect chemical mechanisms (Yan et al., 2019). Nevertheless, the model can reproduce the evolution of each severe particle pollution episode well, including the accumulation of pollutants, the continuing process and the gradual dissipation of pollution.

Table 2

Figure S7/S8 shows the modeled spatial distribution of $PM_{2.5}$, sulfate, nitrate and ammonium concentrations for the four typical heavy pollution processes over Jingzhou/China. The spatial distribution of the three inorganic salts is similar to that of $PM_{2.5}$. Over Central China, the main components of $PM_{2.5}$ are the three inorganic salts in these pollution episodes, with the averaged contributions of sulfate, nitrate and ammonium being ~20%, ~18% and ~13%, respectively. Huang et al. (2014) have also reported that the three secondary inorganic particles rank the highest fraction among the $PM_{2.5}$ species in Central-Eastern China. As Table 3 shown, in addition to inorganic salts, other chemical components include dust (~15%), black carbon (~7%), primary organic aerosol (~14%) and second organic aerosol (~13%).

Table 3

In these four pollution events, the differences in mass percentages of each chemical component ranged from 0.1% (dust) to 6.2% (sulfate) (Table 3). Spatial distribution of $PM_{2.5}$, sulfate, nitrate and ammonium concentrations averaged in the four typical heavy pollution processes over Jingzhou/China are shown in Fig. S7/S8. See details in Sect. 3.4 for further analysis of the causes for the differences.

3.4 Local emissions versus transportation contributions to $PM_{2.5}$ under the four main PSC

In order to investigate the effectiveness of emission control to reduce $PM_{2.5}$ pollution of Central China in the four typical severe particle pollution episodes, firstly we estimate the local sources versus transportation contributions of $PM_{2.5}$ by GEOS-Chem sensitivity simulations (Table 2). Results of XJ0 indicates the contribution of local emission sources to the $PM_{2.5}$ pollution over Jingzhou. The difference between CON and XCC0 shows the transportation contribution of $PM_{2.5}$ outside Central China to Jingzhou. The difference between CON and NCP0/YRD0/PRD0/SCB0 represents the contribution of pollution transportation from NCP/YRD/PRD/SCB regions to Jingzhou.

Figure 6

For the SW-type synoptic situation, differences between the simulation results of NCP0/YRD0/SCB0 and CON show that pollution controlled by SW-type circulation over Central China is almost not affected by the emission sources from North China/East China/Sichuan Basin. The concentrations of $PM_{2.5}$ and three inorganic salts simulated by NCP0/YRD0/SCB0 are similar to those simulated by CON, with a difference less than 3.0% (Fig. 7). However, affected by the southerly airflow at 850 hPa (Fig. 6), air pollutants formed over southern China could be transmitted to Central China, with the transportation contribution of 7.6%. In addition, the contributions from

https://doi.org/10.5194/acp-2020-920
Preprint. Discussion started: 14 November 2020

transboundary transport from non-Jingzhou Central China is simulated to be 12.0%. The transportation of air pollutants from the south makes the proportion of the three inorganic salts (45.7%) in Jingzhou area the smallest among the four pollution episodes (50.3%-55.5% for other three episodes), because the emissions of SO_2, NO_2 and NH_3 in the south (especially in Guangxi and Guizhou province) are smaller than those in Central China (Li et al., 2017a). Associated with the small surface wind speed of 2.1 m/s on average (Fig. 5) and the weak ascending in the vertical direction (Fig. 6) at Jingzhou, it is not conducive to the dispersion of local pollutants (Zheng et al., 2015). The high $PM_{2.5}$ concentrations are mainly accumulated by local emissions. The simulations of XJ0 and CON show that the local emission sources over Jingzhou contribute ~70% to $PM_{2.5}$.

Figure 7

Figure 8

For the NW-type synoptic mode, affected by the northerly airflow (Fig. 8), it is conducive to the southward movement of air pollutants in northern China (He et al., 2018; Leung et al., 2018). Influenced by the local and surrounding terrain over Central China (Fig. 1), two transportation channels are formed from north to south and from northeast to southwest (Fig. 8). In addition, due to the local small wind speed (1.4 m/s on average) near the ground (Fig. 5), the weak convection and the warm ridge along the East Asia coast (Fig. 8), the local and transported pollutants accumulate in Central China. The average concentration of $PM_{2.5}$ in Jingzhou is 179.4 μg/m^3. Due to the transportation contribution of pollutants from northern China (with much higher anthropogenic emissions of SO_2, NO_2 and NH_3) (Li et al., 2017a), the total proportion of the three inorganic salts is the highest (55.5%). The $PM_{2.5}$ concentration simulated in NCP0 is 63.1% of that by CON simulation (Fig. 7), indicating that the transportation

https://doi.org/10.5194/acp-2020-920
Preprint. Discussion started: 14 November 2020

contribution from North China in this heavy pollution episode is as high as 36.9%. The contribution of local emission sources is much smaller than that of the SW-type synoptic pattern, only 41.2% (comparison between XJ0 and CON).

Figure 9

Under the A-type circulation, Jingzhou is controlled by a high pressure system (Fig. 9) which can lead to stable weather conditions caused by radiation inversion (Guo et al., 2015) and subsidence inversion (Kurita et al., 1985), being favorable to continuous accumulation of local pollutants (Guo et al., 2015). The distribution of $PM_{2.5}$ in China is similar to that of SW-type weather condition, with an averaged $PM_{2.5}$ concentration of 128.6 μg/m^3 over Central China. Unlike SW-type, the $PM_{2.5}$ at Jingzhou in this synoptic pattern is less affected by transboundary transport, with the total transportation contribution of the surrounding four major pollution regions being less than 9%. The contribution of local emission sources is about 82% (Fig. 7).

Figure 10

Under the C-type synoptic pattern, the southwest low pressure center is formed at 850 hPa, and Jingzhou is located in the low pressure system on the SLP field (Fig. 10). In combination with the large relative humidity (78% on average; Fig. 5) because that the occurrence season of C-type is the late winter and early spring, it can promote the haze pollution owing to its impact on hydrophilic aerosols (Twohy et al., 2009; Zheng et al., 2015). Together with the small wind speed (less than 4 m/s; Fig. 5), it is easy to cause the accumulation of pollutants. The average concentration of $PM_{2.5}$ over Central China is as high as 203.7 μg/m^3. Air pollution controlled by this weather condition is the most serious of the four typical synoptic controls. However, in this weather situation, pollutants in North China are easy to diffuse (Miao et al., 2017; Li et al., 2019), and the

https://doi.org/10.5194/acp-2020-920
Preprint. Discussion started: 14 November 2020

concentration of $PM_{2.5}$ is significantly lower than that in the former three weather situations (Fig. 10 and Fig. S8). The contribution of pollution transport from non-Central China region simulated by GEOS-Chem is less than 8%, and the contribution of local emission sources at Jingzhou is more than 85% (Fig. 7).

3.5 Effectiveness of emission reduction under the four main PSC

In order to estimate the effectiveness of emission reduction in severe pollution events forced by the four potential synoptic controls, we conduct sensitivity simulations by applying seven emission scenarios (Table 2). All emission scenarios use the reduction ratio of 20% which is close to the average of the target emission reduction of all provinces in the 13th Five-year plan (The State Council of the People's Republic of China, 2016). The differences in model results between CON and JSN/JSNN/JALL represent the environmental benefits caused by different local emission reduction scenarios. The potential $PM_{2.5}$ mitigations by joint prevention and control in different regions are calculated by sensitivity experiments of CCALL, CNALL, CPALL and TALL.

In the JSN emission reduction scenario, the sulfate and ammonium concentrations over Jingzhou are significantly reduced by 3.2-5.8 μg/m^3 (12.7-14.5%) and 0.6-1.9 μg/m^3 (3.2-5.9%) in these four pollution events, respectively. However, the concentration of nitrate increases (1.3-1.7%). This is because there is a competition mechanism between nitrate and sulfate. Ammonium ions always react with sulfate ions first to generate ammonium sulfate, which will continue to react with nitrate ions to generate ammonium nitrate when ammonium ions are rich (Mao et al., 2010). The modeling results indicate that there are enough NH_3 emissions over Central China to consume all sulfate ions, but not enough to combine with all nitrate ions. Thus the reduction of SO_2 emission increases the concentration of nitrate, which offset the contribution of sulfate particle reduction to the environment to some extent. Therefore, the application of JSN emission reduction scheme only reduces the $PM_{2.5}$

https://doi.org/10.5194/acp-2020-920
Preprint. Discussion started: 14 November 2020

concentrations by 3.1-7.2 μg/m^3 (2.0-3.5%, Fig. 11). This inefficient emission reduction scheme is most widely used in heavy pollution areas over China in the past decade, ignoring the synergistic effect of various precursors.

Figure 11

By applying the JSNN and JALL emission reduction scenarios, we aim to evaluate the synergistic effect of multiple precursors on emission reduction. These two scenarios reduce the average sulfate concentration in Jingzhou by 2.8-6.7 μg/m^3 (11.3-17.3%) and 2.9-7.2 μg/m^3 (11.7-17.9%), and the ammonium concentration by 2.0-4.8 μg/m^3 (12.1-16.5%) and 2.2-4.7 μg/m^3 (13.2-17.3%), respectively. Unlike the increments of nitrate in JSN emission reduction scenario, the nitrate decreases (JSNN: 0.3-1.2 μg/m^3; JALL: 0.4-1.5 μg/m^3). Therefore, through the application of JSNN and JALL emission reduction schemes, $PM_{2.5}$ concentrations decrease by 4.9-8.3% and 9.0-15.9%, respectively (Fig. 11), much higher than the improvement by JSN scenario. Zheng et al. (2019b) has also evaluated the sensitiveness of NH_3 control to $PM_{2.5}$ reduction based on observations. However, these results indicate that it is unrealistic to substantially reduce local emissions to achieve the national air quality standard in the long term.

Additionally, the sensitivity simulations by excluding emission sources over upwind regions are conducted to estimate the potential $PM_{2.5}$ mitigations of inter-regional and intra-regional joint control. Our results show that after applying TALL emission reduction scenario, $PM_{2.5}$ concentrations have been significantly improved, with the improvement rates increased from 9.0-15.9% (by JALL scenario) to 17.4-18.8% (Fig. 11). Especially, the NW-type synoptic controlled air pollution episode shows the best effect of joint prevention, followed by SW-type. For NW-type, by reducing emissions over Central China and Northern China (CNALL scheme), $PM_{2.5}$ concentrations are reduced by 26.5 μg/m^3 (16.9%), much more effective than JALL emission reduction scheme (14.1 μg/m^3, 9.0%). In SW-type controlled pollution episode, it should be otherwise to decrease the emissions over Southern China in addition to Central China.

4. Conclusion

The $PM_{2.5}$ pollution in autumn and winter haze periods is now the key obstacle for further improving the air quality in China. The extremely severe and persistent $PM_{2.5}$ pollution episodes are attributed to dominant synoptic conditions in addition to high precursor emissions. For the $PM_{2.5}$ mitigations during winter haze episodes in specific region forced by potential synoptic controls, how to effectively reduce emissions has become an urgent scientific question to be answered. Our results over Central China could provide reference for regional air quality policy-making.

Through Lamb-Jenkension circulation classification, the top four potential synoptic controls (PSC) of heavy $PM_{2.5}$ pollution days (totally 109 days) over Central China from 2013 to 2018 are decomposed to be SW-type, NW-type A-type and C-type, accounting for 29%, 27%, 19% and 12% of the total pollution days, respectively. In these four PSC, three inorganic salt aerosols (sulfate: ~20%; nitrate: ~18%; ammonium: ~13%) totally accounted for ~51% of $PM_{2.5}$ concentrations simulated by optimized GEOS-Chem modelling. The difference of $PM_{2.5}$ concentrations for the four PSC is mainly contributed by the differences of the three inorganic salts.

In the SW-type/NW-type synoptic situation, affected by the southerly/northerly airflow, pollutants over southern/northern China could be transmitted to Central China, with the transportation contribution of 7.6%/37%. In the situation A-type/C-type weather, affected by stable weather condition/high relative humidity, the pollution processes are less affected by the emission sources from non-local regions. And the local emission sources contribute 82%/85% of $PM_{2.5}$.

By only reducing SO_2 and NO_x emission and not controlling NH_3, due to the competition mechanism between nitrate and sulfate, the concentrations of sulfate and ammonium decrease, but the concentration of nitrate increase instead. The enhanced nitrate counteracts the effect of sulfate reduction on $PM_{2.5}$ mitigation with less than 4% decrease in $PM_{2.5}$. Even if the NH_3 emission is also reduced, the $PM_{2.5}$ concentration reduction is less than 9%. By applying the TALL emission reduction scenario, $PM_{2.5}$ concentrations would decrease significantly, with the improvement rate increased from 9.0-15.9% (by JALL scenario) to 17.4-18.8%.

These results provide an opportunity to effectively mitigate haze pollution by local emission control actions in coordination with regional collaborative actions according to different synoptic patterns. Especially, the NW-type synoptic controlled air pollution episode shows the best effect of joint prevention, followed by SW-type. It is noted that in this study, the division of transmission areas is relatively rough, and more accurate source area identification and refined assessment of emission reduction effect of multiple pollutants from source groups are needed in the follow-up.

Acknowledgement

This study was financially supported by the National Natural Science Foundation of China (41830965; 41775115; 41905112), the Key Program of Ministry of Science and Technology of the People’s Republic of China (2017YFC0212602; 2016YFA0602002), the Key Program for Technical Innovation of Hubei Province (2017ACA089) and the Program for Environmental Protection in Hubei Province (2017HB11). The research was also funded by the Fundamental Research Funds for the Central Universities, China University of Geosciences (Wuhan) (G1323519230; 201616; 26420180020; CUG190609) and the Start-up Foundation for Advanced Talents (162301182756).

Author contributions

Yingying Yan and Shaofei Kong conceived and designed the research. Yingying Yan performed the data processing, model simulations, and analyses. Yue Zhou assisted in the circulation classification. Jian Wu provided the emission data over

Central China. Shaofei Kong, Tianliang Zhao and Dantong Liu contributed the funding acquisition. Yingying Yan wrote the paper with input from all authors.

Data availability

Observational data are obtained from individual sources (see links in the text). Model results are available upon request. Model codes are available on a collaborative basis.

Competing interests

The authors declare that they have no conflict of interest.

References

The People's Government of Beijing Municipality (PGBM): Emergency plan for severe air pollution in Beijing, available at: http://www.beijing.gov.cn/zhengce/zhengcefagui/201905/t20190522_61613.html (last access: 14 July 2018), 2018 (in Chinese).

The People's Government of Guangdong Province (PGGP): Emergency plan for severe air pollution in Pearl River Delta, available at: http://www.gd.gov.cn/gkmlpt/content/0/142/post_142657.html#7 (last access: 14 July 2018), 2014 (in Chinese).

The People's Government of Shanghai Municipality (PGSM): Special emergency plan for heavy air pollution in Shanghai, available at: http://www.shanghai.gov.cn/nw2/nw2314/nw2319/nw31973/nw32019/nw32022/nw32023/u21aw1316153.html (last access: 14 July 2018), 2018 (in Chinese).

The State Council of the People's Republic of China (SCPPC): The Thirteenth Five-Year Plan for Energy Saving and Emission Reduction, available at: http://www.gov.cn/gongbao/content/2017/content_5163448.htm (last access: 14 July 2018), 2016 (in Chinese).

The State Council of the People's Republic of China (SCPPC): Air Pollution Prevention and Control Action Plan, available at: http://www.gov.cn/zhengce/content/2013-09/13/content_4561.htm (last access: 14 July 2018), 2013 (in Chinese).

Jenkinson A. F., Collison F. P.: An initial climatology of gales over the North Sea. Synoptic Climatology Branch Memorandum, 62. Bracknell: Meteorological Office, 1-18, 1977.

Lamb H H. Types and spells of weather around the year in the British Isles. Quarterly Journal Royal Meteorological Society, 76, 393-438, 1950.

Agarwal, N. K., Sharma, P., and Agarwal, S. K.: Particulate matter air pollution and cardiovascular disease, Medical Science, 21, 270-279, 2017.

An, Z., Huang, R.J., Zhang, R., Tie, X., Li, G., Cao, J., Zhou, W., Shi, Z., Han, Y., Gu, Z., and Ji, Y.: Severe haze in northern China: A synergy of anthropogenic emissions and atmospheric processes, Proceedings of the National Academy of Sciences of the United States of America, 116, 8657-8666, 10.1073/pnas.1900125116, 2019.

Bei, N., Zhao, L., Xiao, B., Meng, N., and Feng, T.: Impacts of local circulations on the wintertime air pollution in the Guanzhong Basin, China, Science of the Total Environment, 592, 373-390, 10.1016/j.scitotenv.2017.02.151, 2017.

Bi, X., Dai, Q., Wu, J., Zhang, Q., Zhang, W., Luo, R., Cheng, Y., Zhang, J., Wang, L., Yu, Z., Zhang, Y., Tian, Y., and Feng, Y.: Characteristics of the main primary source profiles of particulate matter across China from 1987 to 2017, Atmospheric Chemistry and Physics, 19, 3223-3243, 10.5194/acp-19-3223-2019, 2019.

Cheng, J., Su, J., Cui, T., Li, X., Dong, X., Sun, F., Yang, Y., Tong, D., Zheng, Y., Li, Y., Li, J., Zhang, Q., and He, K.: Dominant role of emission reduction in $PM_{2.5}$ air quality improvement in Beijing during 2013-2017: a model-based decomposition analysis, Atmospheric Chemistry and Physics, 19, 6125-6146, 10.5194/acp-19-6125-2019, 2019.

Cheng, Z., Luo, L., Wang, S., Wang, Y., Sharma, S., Shimadera, H., Wang, X., Bressi, M., de Miranda, R. M., Jiang, J., Zhou, W., Fajardo, O., Yan, N., and Hao, J.: Status and characteristics of ambient $PM_{2.5}$ pollution in global megacities, Environment International, 89-90, 212-221, 10.1016/j.envint.2016.02.003, 2016.

Chuang, M.T., Chiang, P.C., Chan, C.C., Wang, C.F., Chang, E. E., and Lee, C.T.: The effects of synoptical weather pattern and complex terrain on the formation of aerosol events in the Greater Taipei area, Science of the Total Environment, 399, 128-146, 10.1016/j.scitotenv.2008.01.051, 2008.

Geng, G., Xiao, Q., Zheng, Y., Tong, D., Zhang, Y., Zhang, X., Zhang, Q., He, K., and Liu, Y.: Impact of China's Air Pollution Prevention and Control Action Plan on $PM_{2.5}$ chemical composition over eastern China, Science China-Earth Sciences, 62, 1872-1884, 10.1007/s11430-018-9353-x, 2019.

Gong, W., Zhang, T., Zhu, Z., Ma, Y., Ma, X., and Wang, W.: Characteristics of $PM_{1.0}$, $PM_{2.5}$, and PM_{10}, and Their Relation to Black Carbon in Wuhan, Central China, Atmosphere, 6, 1377-1387, 10.3390/atmos6091377, 2015.

Guo, L., Guo, X., Fang, C., and Zhu, S.: Observation analysis on characteristics of formation, evolution and transition of a long-lasting severe fog and haze episode in North China, Science China-Earth Sciences, 58, 329-344, 10.1007/s11430-014-4924-2, 2015.

He, J., Gong, S., Zhou, C., Lu, S., Wu, L., Chen, Y., Yu, Y., Zhao, S., Yu, L., and Yin, C.: Analyses of winter circulation types and their impacts on haze pollution in Beijing, Atmospheric Environment, 192, 94-103, 10.1016/j.atmosenv.2018.08.060, 2018.

Huang, R.J., Zhang, Y., Bozzetti, C., Ho, K.F., Cao, J.J., Han, Y., Daellenbach, K. R., Slowik, J. G., Platt, S. M., Canonaco, F., Zotter, P., Wolf, R., Pieber, S. M., Bruns, E. A., Crippa, M., Ciarelli, G., Piazzalunga, A., Schwikowski, M., Abbaszade, G., Schnelle-Kreis, J., Zimmermann, R., An, Z., Szidat, S., Baltensperger, U., El Haddad, I., and Prevot, A. S. H.: High secondary aerosol contribution to particulate pollution during haze events in China, Nature, 514, 218-222, 10.1038/nature13774, 2014.

https://doi.org/10.5194/acp-2020-920
Preprint. Discussion started: 14 November 2020

Atmospheric Chemistry and Physics Discussions
Open Access
EGU

Huang, X., Ding, A., Gao, J., Zheng, B., Zhou, D., Qi, X., Tang, R., Wang, J., Ren, C., Nie, W., Chi, X., Xu, Z., Chen, L., Li, Y., Che, F., Pang, N., Wang, H., Tong, D., Qin, W., Cheng, W., Liu, W., Fu, Q., Liu, B., Chai, F., Davis, S. J., Zhang, Q., and He, K.: Enhanced secondary pollution offset reduction of primary emissions during COVID-19 lockdown in China, National Science Review, 10.1093/nsr/nwaa137, 2020.

Kurita, H., Sasaki, K., Muroga, H., Ueda, H., and Wakamatsu, S.: Long-range transport of air pollution under light gradient wind conditions, Journal of Climate and Applied Meteorology, 24, 425-434, 10.1175/1520-0450(1985)024<0425:lrtoap>2.0.co;2, 1985.

Leung, D. M., Tai, A. P. K., Mickley, L. J., Moch, J. M., van Donkelaar, A., Shen, L., and Martin, R. V.: Synoptic meteorological modes of variability for fine particulate matter ($PM_{2.5}$) air quality in major metropolitan regions of China, Atmospheric Chemistry and Physics, 18, 6733-6748, 10.5194/acp-18-6733-2018, 2018.

Li, J., Liao, H., Hu, J., and Li, N.: Severe particulate pollution days in China during 2013-2018 and the associated typical weather patterns in Beijing-Tianjin-Hebei and the Yangtze River Delta regions, Environmental Pollution, 248, 74-81, 10.1016/j.envpol.2019.01.124, 2019.

Li, M., Zhang, Q., Kurokawa, J.-i., Woo, J.-H., He, K., Lu, Z., Ohara, T., Song, Y., Streets, D. G., Carmichael, G. R., Cheng, Y., Hong, C., Huo, H., Jiang, X., Kang, S., Liu, F., Su, H., and Zheng, B.: MIX: a mosaic Asian anthropogenic emission inventory under the international collaboration framework of the MICS-Asia and HTAP, Atmospheric Chemistry and Physics, 17, 935-963, 10.5194/acp-17-935-2017, 2017a.

Li, X., Zhang, Q., Zhang, Y., Zhang, L., Wang, Y., Zhang, Q., Li, M., Zheng, Y., Geng, G., Wallington, T. J., Han, W., Shen, W., and He, K.: Attribution of $PM_{2.5}$ exposure in Beijing-Tianjin-Hebei region to emissions: implication to control strategies, Science Bulletin, 62, 957-964, 10.1016/j.scib.2017.06.005, 2017b.

Li, Z., Guo, J., Ding, A., Liao, H., Liu, J., Sun, Y., Wang, T., Xue, H., Zhang, H., and Zhu, B.: Aerosol and boundary-layer interactions and impact on air quality, National Science Review, 4, 810-833, 10.1093/nsr/nwx117, 2017c.

Liao, Z., Gao, M., Sun, J., and Fan, S.: The impact of synoptic circulation on air quality and pollution-related human health in the Yangtze River Delta region, Science of the Total Environment, 607, 838-846, 10.1016/j.scitotenv.2017.07.031, 2017.

Liao, Z., Xie, J., Fang, X., Wang, Y., Zhang, Y., Xu, X., and Fan, S.: Modulation of synoptic circulation to dry season $PM_{2.5}$ pollution over the Pearl River Delta region: An investigation based on self-organizing maps, Atmospheric Environment, 230, 10.1016/j.atmosenv.2020.117482, 2020.

Lin, J., Tong, D., Davis, S., Ni, R., Tan, X., Pan, D., Zhao, H., Lu, Z., Streets, D., Feng, T., Zhang, Q., Yan, Y., Hu, Y., Li, J., Liu, Z., Jiang, X., Geng, G., He, K., Huang, Y., and Guan, D.: Global climate forcing of aerosols embodied in international trade, Nature Geoscience, 9, 790-+, 10.1038/ngeo2798, 2016.

Lin, Y., Zou, J., Yang, W., and Li, C.Q.: A Review of Recent Advances in Research on $PM_{2.5}$ in China, International Journal of Environmental Research and Public Health, 15, 10.3390/ijerph15030438, 2018.

Liu, M., Lin, J., Wang, Y., Sun, Y., Zheng, B., Shao, J., Chen, L., Zheng, Y., Chen, J., Fu, T.-M., Yan, Y., Zhang, Q., and Wu, Z.: Spatiotemporal variability of NO_2 and $PM_{2.5}$ over Eastern China: observational and model analyses with a novel statistical method, Atmospheric Chemistry and Physics, 18, 12933-12952, 10.5194/acp-18-12933-2018, 2018.

Liu, M., Huang, X., Song, Y., Tang, J., Cao, J., Zhang, X., Zhang, Q., Wang, S., Xu, T., Kang, L., Cai, X., Zhang, H., Yang, F., Wang, H., Yu, J. Z., Lau, A. K. H., He, L., Huang, X., Duan, L., Ding, A., Xue, L., Gao, J., Liu, B., and Zhu, T.: Ammonia emission control in China would mitigate haze pollution and nitrogen deposition, but worsen acid rain, Proceedings of the National Academy of Sciences of the United States of America, 116, 7760-7765, 10.1073/pnas.1814880116, 2019.

Mao, J., Jacob, D. J., Evans, M. J., Olson, J. R., Ren, X., Brune, W. H., Clair, J. M. S., Crounse, J. D., Spencer, K. M., Beaver, M. R., Wennberg, P. O., Cubison, M. J., Jimenez, J. L., Fried, A., Weibring, P., Walega, J. G., Hall, S. R., Weinheimer, A. J., Cohen, R. C., Chen, G., Crawford, J. H., McNaughton, C., Clarke, A. D., Jaeglé, L., Fisher, J. A., Yantosca, R. M., Le Sager, P., and Carouge, C.: Chemistry of hydrogen oxide radicals (HOx) in the Arctic troposphere in spring, Atmospheric Chemistry and Physics, 10, 5823-5838, 10.5194/acp-10-5823-2010, 2010.

Miao, Y., Guo, J., Liu, S., Liu, H., Li, Z., Zhang, W., and Zhai, P.: Classification of summertime synoptic patterns in Beijing and their associations with boundary layer structure affecting aerosol pollution, Atmospheric Chemistry and Physics, 17, 3097-3110, 10.5194/acp-17-3097-2017, 2017.

Ning, G., Wang, S., Yim, S. H. L., Li, J., Hu, Y., Shang, Z., Wang, J., and Wang, J.: Impact of low-pressure systems on winter heavy air pollution in the northwest Sichuan Basin, China, Atmospheric Chemistry and Physics, 18, 13601-13615, 10.5194/acp-18-13601-2018, 2018.

Pope, R. J., Savage, N. H., Chipperfield, M. P., Ordonez, C., and Neal, L. S.: The influence of synoptic weather regimes on UK air quality: regional model studies of tropospheric column NO_2, Atmospheric Chemistry and Physics, 15, 11201-11215, 10.5194/acp-15-11201-2015, 2015.

Russo, A., Trigo, R. M., Martins, H., and Mendes, M. T.: NO_2, PM_{10} and O_3 urban concentrations and its association with circulation weather types in Portugal, Atmospheric Environment, 89, 768-785, 10.1016/j.atmosenv.2014.02.010, 2014.

Shu, L., Xie, M., Gao, D., Wang, T., Fang, D., Liu, Q., Huang, A., and Peng, L.: Regional severe particle pollution and its association with synoptic weather patterns in the Yangtze River Delta region, China, Atmospheric Chemistry and Physics, 17, 12871-12891, 10.5194/acp-17-12871-2017, 2017.

Sun, Y., Niu, T., He, J., Ma, Z., Liu, P., Xiao, D., Hu, J., Yang, J., and Yan, X.: Classification of circulation patterns during the formation and dissipation of

https://doi.org/10.5194/acp-2020-920
Preprint. Discussion started: 14 November 2020

continuous pollution weather over the Sichuan Basin, China, Atmospheric Environment, 223, 10.1016/j.atmosenv.2019.117244, 2020.

Sun, Y. L., Chen, C., Zhang, Y. J., Xu, W. Q., Zhou, L. B., Cheng, X. L., Zheng, H. T., Ji, D. S., Li, J., Tang, X., Fu, P. Q., and Wang, Z. F.: Rapid formation and evolution of an extreme haze episode in Northern China during winter 2015, Scientific Reports, 6, 10.1038/srep27151, 2016.

Tian, S. L., Pan, Y. P., and Wang, Y. S.: Size-resolved source apportionment of particulate matter in urban Beijing during haze and non-haze episodes, Atmospheric Chemistry and Physics, 16, 1-19, 10.5194/acp-16-1-2016, 2016.

Trigo, R. M., and DaCamara, C. C.: Circulation weather types and their influence on the precipitation regime in Portugal, International Journal of Climatology, 20, 1559-1581, 10.1002/1097-0088(20001115)20:13<1559::aid-joc555>3.0.co;2-5, 2000.

Twohy, C. H., Coakley, J. A., Jr., and Tahnk, W. R.: Effect of changes in relative humidity on aerosol scattering near clouds, Journal of Geophysical Research-Atmospheres, 114, 10.1029/2008jd010991, 2009.

Wang, X., Wei, W., Cheng, S., Li, J., Zhang, H., and Lv, Z.: Characteristics and classification of $PM_{2.5}$ pollution episodes in Beijing from 2013 to 2015, Science of the Total Environment, 612, 170-179, 10.1016/j.scitotenv.2017.08.206, 2018.

Wang, Y., Chen, Y., Wu, Z., Shang, D., Bian, Y., Du, Z., Schmitt, S. H., Su, R., Gkatzelis, G. I., Schlag, P., Hohaus, T., Voliotis, A., Lu, K., Zen, L., Zhao, C., Alfarra, M. R., McFiggans, G., Wiedensohler, A., Kiendler-Scharr, A., Zhang, Y., and Hu, M.: Mutual promotion between aerosol particle liquid water and particulate nitrate enhancement leads to severe nitrate-dominated particulate matter pollution and low visibility, Atmospheric Chemistry and Physics, 20, 2161-2175, 10.5194/acp-20-2161-2020, 2020.

Wu, J., Kong, S., Wu, F., Cheng, Y., Zheng, S., Yan, Q., Zheng, H., Yang, G., Zheng, M., Liu, D., Zhao, D., and Qi, S.: Estimating the open biomass burning emissions in central and eastern China from 2003 to 2015 based on satellite observation, Atmospheric Chemistry and Physics, 18, 11623-11646, 10.5194/acp-18-11623-2018, 2018.

Xu, G., Jiao, L., Zhang, B., Zhao, S., Yuan, M., Gu, Y., Liu, J., and Tang, X.: Spatial and temporal variability of the $PM_{2.5}/PM_{10}$ ratio in Wuhan, Central China, Aerosol and Air Quality Research, 17, 741-751, 10.4209/aaqr.2016.09.0406, 2017.

Yan, Q., Kong, S., Yan, Y., Liu, H., Wang, W., Chen, K., Yin, Y., Zheng, H., Wu, J., Yao, L., Zeng, X., Cheng, Y., Zheng, S., Wu, F., Niu, Z., Zhang, Y., Zheng, M., Zhao, D., Liu, D., and Qi, S.: Emission and simulation of primary fine and submicron particles and water-soluble ions from domestic coal combustion in China, Atmospheric Environment, 224, 10.1016/j.atmosenv.2020.117308, 2020.

Yan, Y., Cabrera-Perez, D., Lin, J., Pozzer, A., Hu, L., Millet, D. B., Porter, W. C., and Lelieveld, J.: Global tropospheric effects of aromatic chemistry with the SAPRC-11 mechanism implemented in GEOS-Chem version 9-02, Geoscientific Model Development, 12, 111-130, 10.5194/gmd-12-111-2019, 2019.

Yan, Y. Y., Lin, J. T., Kuang, Y., Yang, D., and Zhang, L.: Tropospheric carbon monoxide over the Pacific during HIPPO: two-way coupled simulation of GEOS-Chem and its multiple nested models, Atmospheric Chemistry and Physics, 14, 12649-12663, 10.5194/acp-14-12649-2014, 2014.

Yang, Y., Zheng, X., Gao, Z., Wang, H., Wang, T., Li, Y., Lau, G. N. C., and Yim, S. H. L.: Long-term trends of persistent synoptic circulation events in planetary boundary layer and their relationships with haze pollution in winter half year over Eastern China, Journal of Geophysical Research-Atmospheres, 123, 10991-11007, 10.1029/2018jd028982, 2018.

Yu, C., Zhao, T., Bai, Y., Zhang, L., Kong, S., Yu, X., He, J., Cui, C., Yang, J., You, Y., Ma, G., Wu, M., and Chang, J.: Heavy air pollution with a unique "non-stagnant" atmospheric boundary layer in the Yangtze River middle basin aggravated by regional transport of $PM_{2.5}$ over China, Atmospheric Chemistry and Physics, 20, 7217-7230, 10.5194/acp-20-7217-2020, 2020.

Zhang, J. P., Zhu, T., Zhang, Q. H., Li, C. C., Shu, H. L., Ying, Y., Dai, Z. P., Wang, X., Liu, X. Y., Liang, A. M., Shen, H. X., and Yi, B. Q.: The impact of circulation patterns on regional transport pathways and air quality over Beijing and its surroundings, Atmospheric Chemistry and Physics, 12, 5031-5053, 10.5194/acp-12-5031-2012, 2012.

Zhang, Q., Jiang, X., Tong, D., Davis, S. J., Zhao, H., Geng, G., Feng, T., Zheng, B., Lu, Z., Streets, D. G., Ni, R., Brauer, M., van Donkelaar, A., Martin, R. V., Huo, H., Liu, Z., Pan, D., Kan, H., Yan, Y., Lin, J., He, K., and Guan, D.: Transboundary health impacts of transported global air pollution and international trade, Nature, 543, 10.1038/nature21712, 2017.

Zhang, Q., Zheng, Y., Tong, D., Shao, M., Wang, S., Zhang, Y., Xu, X., Wang, J., He, H., Liu, W., Ding, Y., Lei, Y., Li, J., Wang, Z., Zhang, X., Wang, Y., Cheng, J., Liu, Y., Shi, Q., Yan, L., Geng, G., Hong, C., Li, M., Liu, F., Zheng, B., Cao, J., Ding, A., Gao, J., Fu, Q., Huo, J., Liu, B., Liu, Z., Yang, F., He, K., and Hao, J.: Drivers of improved PM2.5 air quality in China from 2013 to 2017, Proceedings of the National Academy of Sciences of the United States of America, 116, 24463-24469, 10.1073/pnas.1907956116, 2019.

Zheng, B., Tong, D., Li, M., Liu, F., Hong, C., Geng, G., Li, H., Li, X., Peng, L., Qi, J., Yan, L., Zhang, Y., Zhao, H., Zheng, Y., He, K., and Zhang, Q.: Trends in China's anthropogenic emissions since 2010 as the consequence of clean air actions, Atmospheric Chemistry and Physics, 18, 14095-14111, 10.5194/acp-18-14095-2018, 2018.

Zheng, H., Kong, S., Wu, F., Cheng, Y., Niu, Z., Zheng, S., Yang, G., Yao, L., Yan, Q., Wu, J., Zheng, M., Chen, N., Xu, K., Yan, Y., Liu, D., Zhao, D., Zhao, T., Bai, Y., Li, S., and Qi, S.: Intra-regional transport of black carbon between the south edge of the North China Plain and central China during winter haze episodes, Atmospheric Chemistry and Physics, 19, 4499-4516, 10.5194/acp-19-4499-2019, 2019a.

Zheng, M., Wang, Y., Bao, J., Yuan, L., Zheng, H., Yan, Y., Liu, D., Xie, M., and Kong, S.: Initial Cost Barrier of Ammonia Control in Central China, Geophysical Research Letters, 46, 14175-14184, 10.1029/2019gl084351, 2019b.

Zheng, X. Y., Fu, Y. F., Yang, Y. J., and Liu, G. S.: Impact of atmospheric circulations on aerosol distributions in autumn over eastern China: observational evidence, Atmospheric Chemistry and Physics, 15, 12115-12138, 10.5194/acp-15-12115-2015, 2015.

Zhong, J., Zhang, X., Dong, Y., Wang, Y., Liu, C., Wang, J., Zhang, Y., and Che, H.: Feedback effects of boundary-layer meteorological factors on cumulative explosive growth of $PM_{2.5}$ during winter heavy pollution episodes in Beijing from 2013 to 2016, Atmospheric Chemistry and Physics, 18, 247-258, 10.5194/acp-18-247-2018, 2018.

https://doi.org/10.5194/acp-2020-920
Preprint. Discussion started: 14 November 2020

Atmospheric Chemistry and Physics Discussions

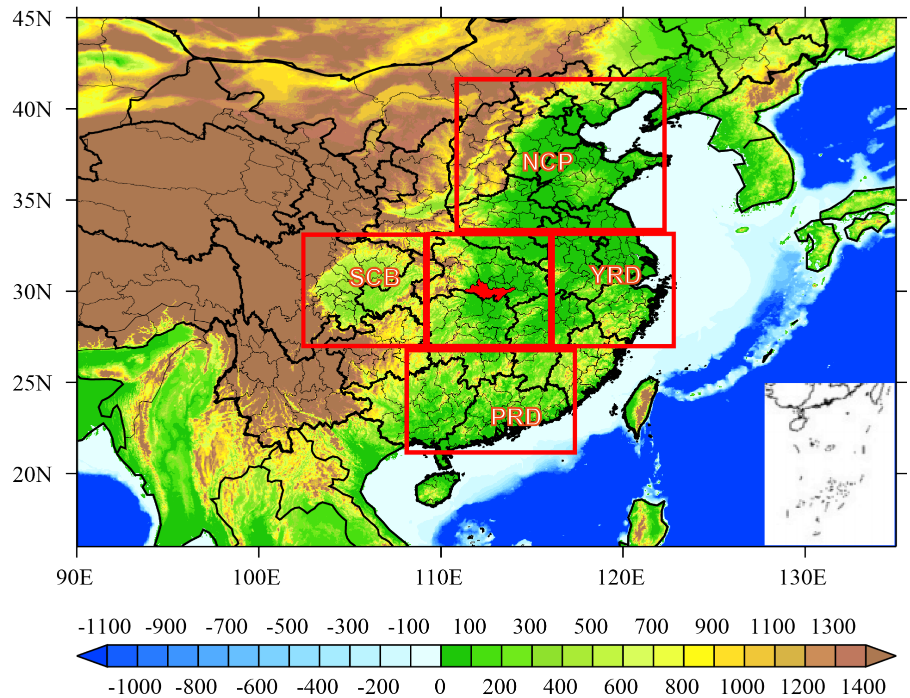

Figue 1 The location of Jingzhou (red area) and the major haze pollution regions of NCP, YRD, PRD, and SCB. The areas framed in red are used to investigate the inter-regional imapcts by GEOS-Chem sensitivity simulations. The overlaid map shows the surface elevation (m) from a 2 min Gridded Global Relief Data (ETOPO2v2) available at NGDC Marine Trackline Geophysical database (http://www.ngdc.noaa.gov/mgg/global/etopo2.html).

https://doi.org/10.5194/acp-2020-920
Preprint. Discussion started: 14 November 2020

Atmospheric Chemistry and Physics Discussions
Open Access
EGU

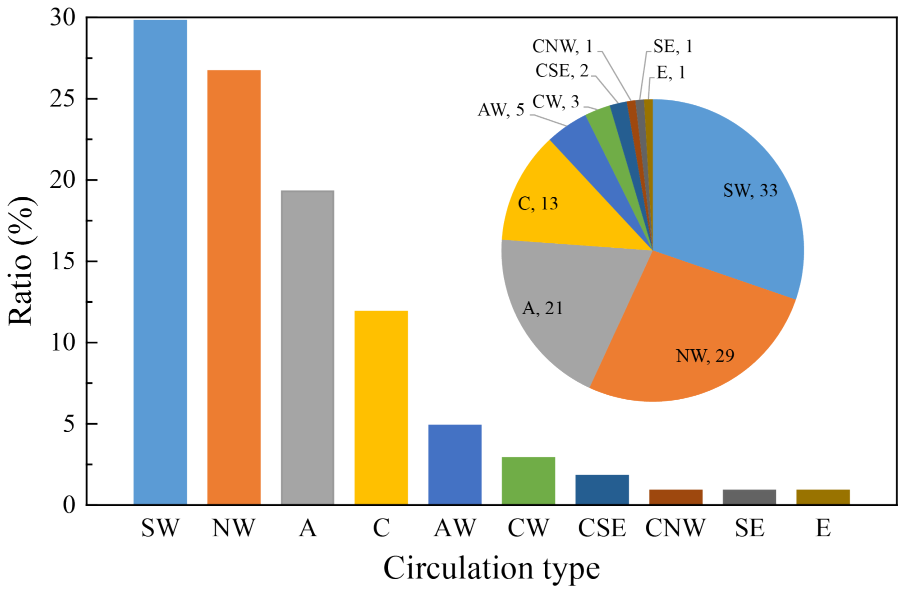

Figure 2 Frequency distributions of ten circulation types for the heavy pollution days of 2013-2018 over Jingzhou. The occurrence numbers of each type are shown. The ten circulation types include Southwest (SW), Northwest (NW), Anticyclone (A), Cyclone (C), Anticyclone-West (AW), Cyclone-West (CW), Cyclone-Southeast (CSE), Cyclone-Northwest (CNW), Southeast (SE) and East (E), respectively.

https://doi.org/10.5194/acp-2020-920
Preprint. Discussion started: 14 November 2020

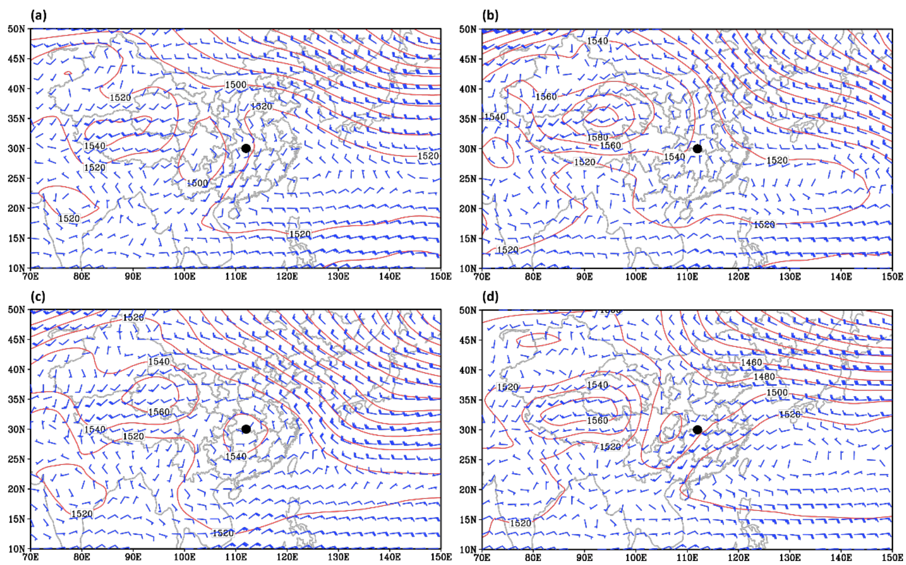

Figure 3 Spatial distribution of 850 hPa geopotential height and wind vector for SW-type (a), NW-type (b), A-type (c) and C-type (d) synoptic control averaged over 2013-2018. The black dot indicates the location of Jingzhou.

https://doi.org/10.5194/acp-2020-920
Preprint. Discussion started: 14 November 2020

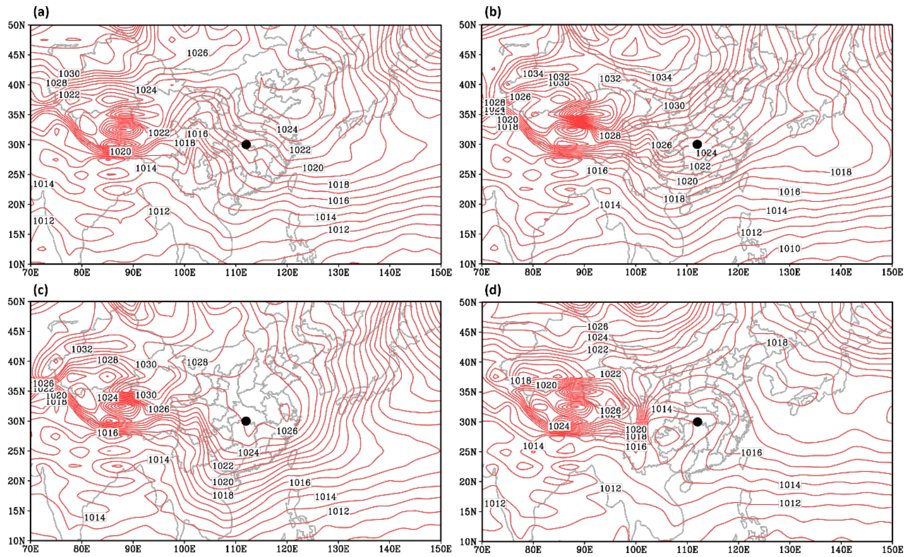

Figure 4 Spatial distribution of sea level pressure for SW-type (a), NW-type (b), A-type (c) and C-type (d) synoptic control averaged over 2013-2018. The black dot indicates the location of Jingzhou.

https://doi.org/10.5194/acp-2020-920
Preprint. Discussion started: 14 November 2020

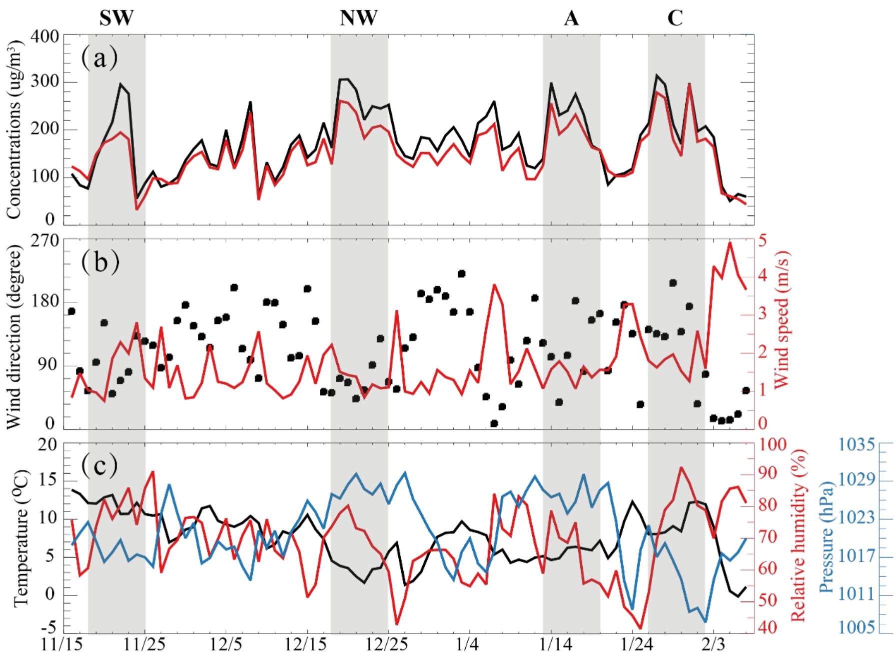

Figure 5 (a) Daily mean values of modeled (red line) and observed (black line) $PM_{2.5}$ concentration ($\mu g/m^3$) at Jingzhou and four severe pollution events (grey area) from November, 2013 to February, 2014. (b) Observed daily mean wind speed (red line) and wind direction (black dots). (c) Obseved temperature (black line), relative humidity (red line) and sea level pressure (blue line).

https://doi.org/10.5194/acp-2020-920
Preprint. Discussion started: 14 November 2020

Atmospheric Chemistry and Physics
Discussions

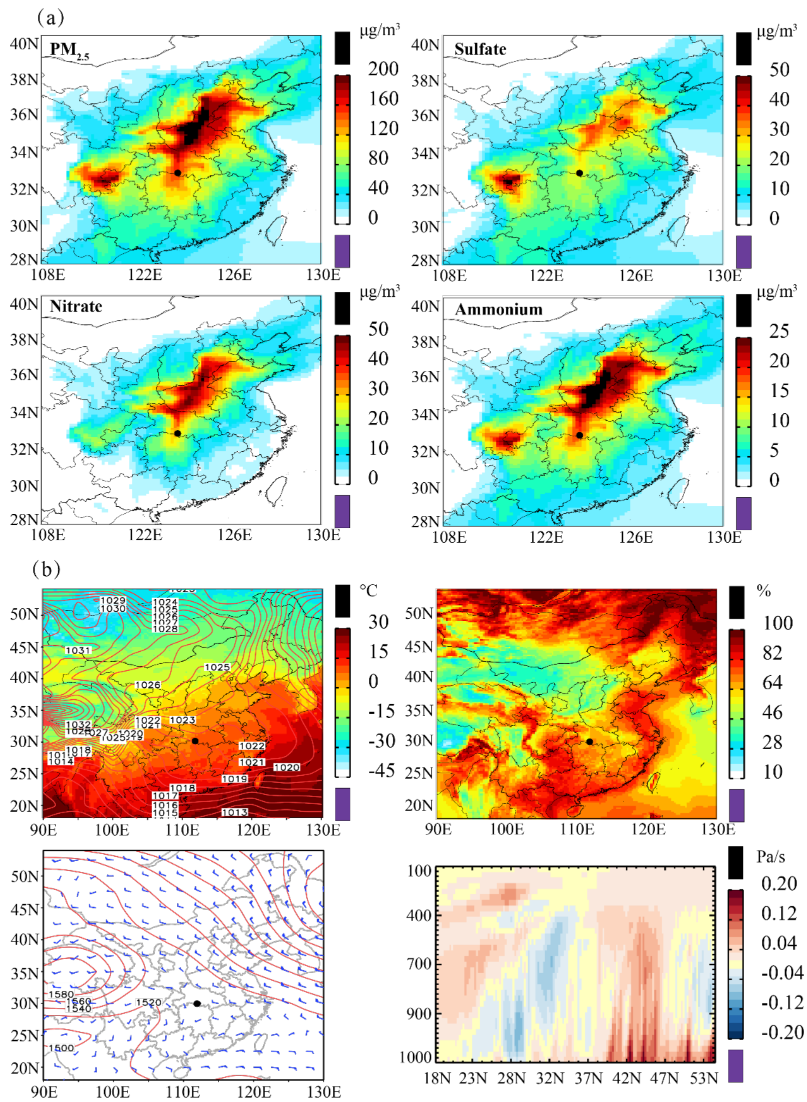

Figure 6 (a) Spatial distribution of $PM_{2.5}$, sulfate, nitrate and ammonium concentrations averaged over SW-type synoptic controls (18-25 November, 2013) simulated by GEOS-Chem control simulation (μg/m^3). (b) Meteorological conditions of SW-type: sea level pressure (red line) and temperature (colour shades), surface relative humidity (%) fields, 850 hPa wind and geopotential height (red line) and height–latitude cross-sections of vertical velocity (Pa/s).

https://doi.org/10.5194/acp-2020-920
Preprint. Discussion started: 14 November 2020

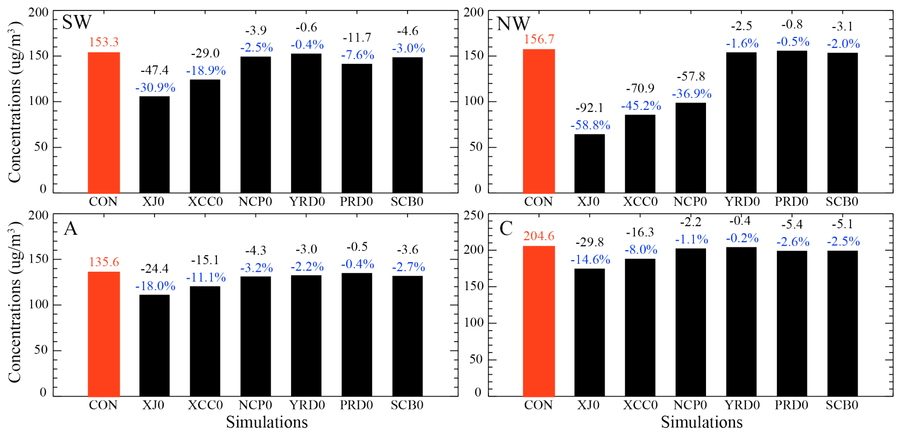

Figure 7 Modeled concentrations (μg/m^3) of $PM_{2.5}$ at Jingzhou in the GEOS-Chem control (red bar) and sensitivity (black bar) simulations in view of the regional transportation, and the differences (black characters for mass concentrations and blue characters for mass percentages) between the sensitivity and the control simulations. The abbreviations of each simulation referred to Table 2.

https://doi.org/10.5194/acp-2020-920
Preprint. Discussion started: 14 November 2020

Atmospheric Chemistry and Physics
Open Access
EGU
Discussions

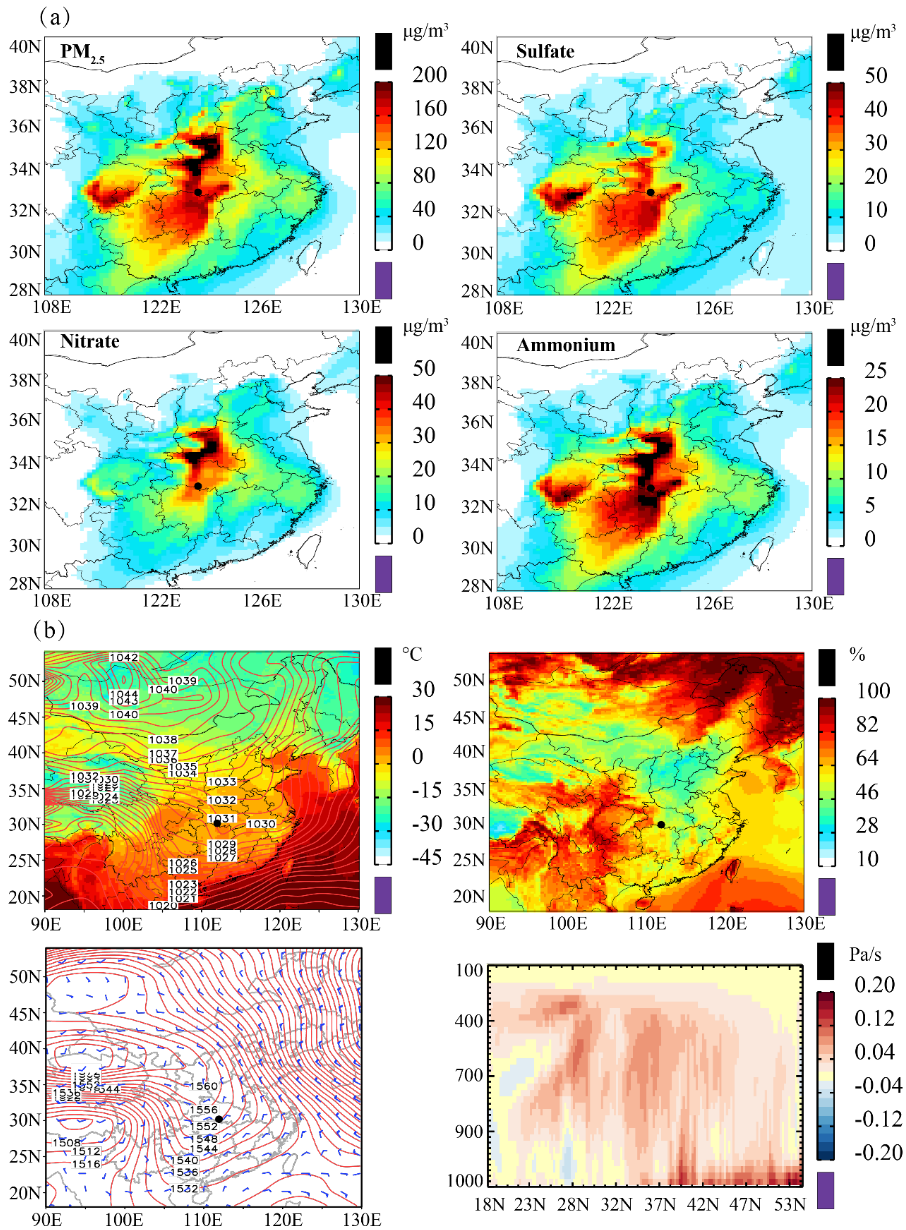

Figure 8 As in Fig. 6 but for NW-type synoptic control (19-26 December, 2013).

https://doi.org/10.5194/acp-2020-920
Preprint. Discussion started: 14 November 2020

Atmospheric Chemistry and Physics
Discussions

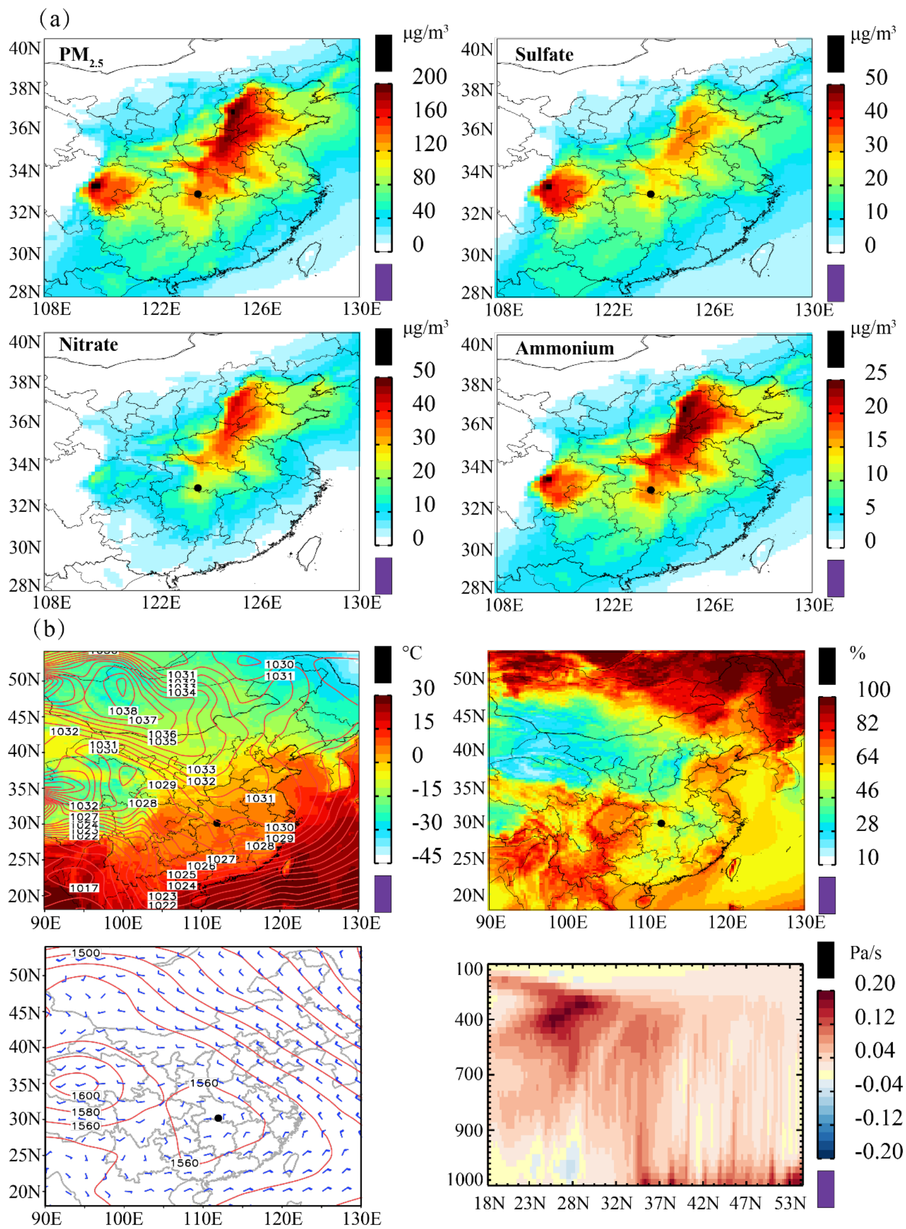

Figure 9 As in Fig. 6 but for A-type synoptic control (14-21 January, 2014).

https://doi.org/10.5194/acp-2020-920
Preprint. Discussion started: 14 November 2020

Atmospheric Chemistry and Physics
Discussions

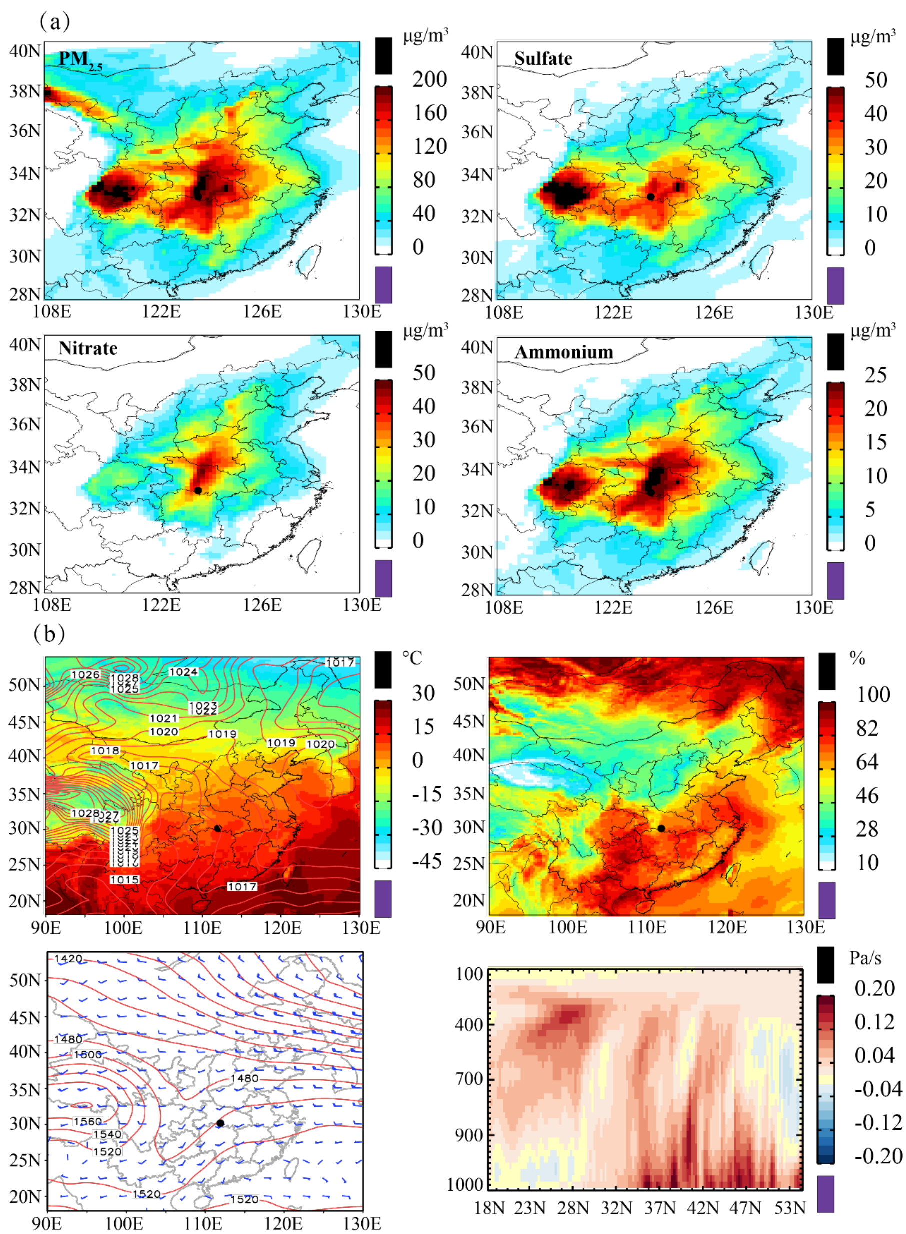

Figure 10 As in Fig. 6 but for C-type synoptic control (26 January - 2 February, 2014).

https://doi.org/10.5194/acp-2020-920
Preprint. Discussion started: 14 November 2020

Atmospheric Chemistry and Physics Discussions

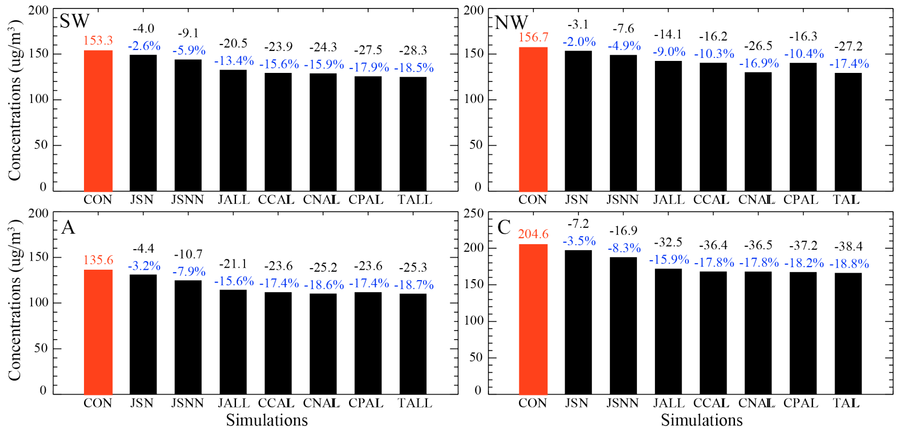

Figure 11 Modeled concentrations (μg/m^3) of $PM_{2.5}$ at Jingzhou in the GEOS-Chem control (red bar) and sensitivity (black bar) simulations for emission reduction, and the differences (black characters for mass concentrations and blue characters for mass percentages) between the sensitivity and the control simulations. The abbreviations of each simulation referred to Table 2.

https://doi.org/10.5194/acp-2020-920
Preprint. Discussion started: 14 November 2020

Atmospheric Chemistry and Physics Discussions
Open Access
EGU

Table 1 Lamb-Jenkinson circulation types

$\lvert\xi\rvert \leq V$ (Flat airflow type)	$\lvert\xi\rvert \geq 2V$ (Rotating airflow type)	$V < \lvert\xi\rvert < 2V$ (Mixed type)
East (E),	Anticyclone (A),	Cyclone-Southeast (CSE),
Southeast (SE),	Cyclone (C)	Cyclone-West (CW),
Southwest (SW),		Cyclone-Northwest (CNW),
Northwest (NW)		Anticyclone-West (AW)

https://doi.org/10.5194/acp-2020-920
Preprint. Discussion started: 14 November 2020

Atmospheric Chemistry and Physics Discussions
Open Access
EGU

Table 2 Description of sensitivity simulations by GEOS-Chem model. The NCP, YRD, PRD and SCB are the areas framed in red showed by Fig. 1.

Simulations	Description
CON	Applying the original emission situation in Table S1
XJ0	Emissions of all pollution sources[1] outside Jingzhou are set to be zero
XCC0	Emissions of all pollution sources outside Central China are set to be zero
NCP0	Emissions of all pollution sources over NCP region are set to be zero
YRD0	Emissions of all pollution sources over YRD region are set to be zero
PRD0	Emissions of all pollution sources over PRD region are set to be zero
SCB0	Emissions of all pollution sources over SCB region are set to be zero
JSN	Emissions of SO_2 and NO_x at Jingzhou are reduced by 20%
JSNN	Emissions of SO_2, NO_x and NH_3 at Jingzhou are reduced by 20%
JALL	Emissions of all pollution sources at Jingzhou are reduced by 20%
CCALL	Emissions of all pollution sources over Central China are reduced by 20%
CNALL	Emissions of all pollution sources over Central China and NCP region are reduced by 20%
CPALL	Emissions of all pollution sources over Central China and PRD region are reduced by 20%
TALL	Emissions of all pollution sources over Central China, NCP, YRD, PRD and SCB region are reduced by 20%

1. All pollution sources include emissions of SO_2, NO_x, NH_3, CO, BC, OC and NMVOCs.

https://doi.org/10.5194/acp-2020-920
Preprint. Discussion started: 14 November 2020

Table 3 Simulated $PM_{2.5}$ concentrations and associated chemical components averaged for the four typical heavy pollution episodes at Jingzhou. Also shown in brackets are the percentages of each component in $PM_{2.5}$.

$PM_{2.5}$ components	Typical heavy pollution episodes			
μg/m^3	11/18-11/25（SW-type）	12/19-12/26（NW-type）	1/14-1/21（A-type）	1/26-2/2（C-type）
Nitrate	30.6 (20.0%)	34.6 (22.1%)	23.4 (17.3%)	42.3 (20.7%)
Sulfate	26.5 (13.4%)	30.7 (19.6%)	27.7 (20.4%)	40.4 (19.7%)
Ammonium	18.8 (12.3%)	21.6 (13.8%)	17.1 (12.6%)	27.1 (13.2%)
Dust	24.4 (15.9%)	22.3 (14.2%)	19.8 (14.6%)	29.2 (14.3%)
BC	10.5 (6.8%)	9.6 (6.1%)	9.5 (7.0%)	13.8 (6.7%)
POA	21.6 (14.1%)	18.9 (12.1%)	18.9 (13.9%)	27.7 (13.5%)
SOA	20.9 (13.6%)	19.0 (12.1%)	19.2 (14.2%)	24.1 (11.8%)
$PM_{2.5}$	153.3	156.7	135.6	204.6